WIRELESS AND STAND-ALONE SUBMARINE PROPELLER BASED ON ACOUSTIC PROPULSION

Jaehoon Lee and Eun Sok Kim

Department of Electrical and Computer Engineering
University of Southern California, Los Angeles, CA 90089, USA

ABSTRACT

This paper presents a wireless and stand-alone subminiature propeller based on acoustic propulsion for the underwater robotic applications. The acoustic propulsion is generated by a MEMSbased self-focusing acoustic transducer (SFAT), fabricated on 1mm-thick lead zirconate titanate (PZT) substrate, and operated at its thickness mode resonant frequency of 2.32 MHz. A 100F lithium-ion capacitor (LIC) is used as a power source due to its high energy and power densities. A drive electronic circuit is implemented on a flexible printed circuit board (PCB) and delivers 30V_{pp} sinusoidal signal to the acoustic propeller. The completed system is 18 x 18 x 38 mm³ in volume and weighs 12.56 grams, resulting in a mass density of 1.020 g/cm³. The acoustic propulsion generated by the acoustic propeller is measured to be 18.68µN with the electrical power of 358.7mW consumed by the propeller. Both vertical and horizontal propulsions are demonstrated successfully in sodium polytungstate (SPT) solution.

KEYWORDS

Acoustic propulsion, Wireless acoustic propeller, Underwater propeller, Self-focusing acoustic transducer, Lithium-ion capacitor.

INTRODUCTION

Underwater robotic systems can perform various tasks such as exploring, salvaging, and delivering in industrial and biomedical environments. Especially, miniaturized robots or microrobots with dimensions in micron scale will be extremely useful for healthcare, as those can deliver drugs and also carry imaging or surgical systems inside human body. Propulsion of underwater robots can be done with a mechanical propelling fan, which is easily worn and torn out, or can potentially damage the surrounding environment with its moving parts. Mimicking fish movement with structures like fish fins can be used for underwater propulsion, but still requires moving parts [1]. On the other hand, a self-focusing

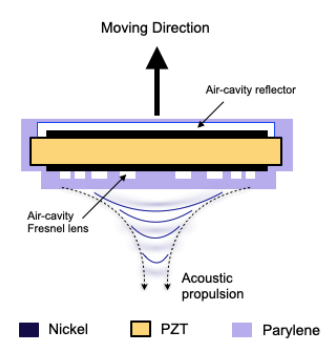


Figure 1: Conceptual illustration of generating acoustic propulsion with a Self-Focusing Acoustic Transducer (SFAT) with air cavity reflector and Fresnel air-cavity lens.

acoustic transducer (SFAT) can generate propulsion force in liquid without any moving parts, as it can produce focused ultrasound capable of acoustic propulsion. Thus, we have developed a SFAT-based underwater acoustic propeller by attaching an air-cavity reflector (made with an acrylic sheet) on the top side of the transducer to allow the waves (generated by SFAT) only on the bottom side of the SFAT, so that there is a net propulsion force directed upward, as illustrated in Fig. 1. Although, we reported an immersive underwater acoustic propeller previously [2], our previous work required electrical wires to deliver electrical power to the SFAT which, by the way, requires relatively high instantaneous power.

In this paper, we present the first acoustic propeller operating free of electrical wires through using a lithium-ion capacitor as the power source. This paper describes the design and fabrication process of the propeller along with the electronic circuits implemented on a flexible printed circuit board (PCB). Also presented are the experiment results in both vertical and horizontal propulsions.

DESIGN AND FABRICATION PROCESSSystem Design

The SFAT-based acoustic propeller integrates four parts on a single stand-alone platform (Fig.2): a self-focusing acoustic transducer for focused ultrasound (2.32MHz), a drive electronics on a flexible printed circuit board, a lithium-ion capacitor (LIC) for power, and a coil for wireless charging of the LIC. The flexible PCB wraps around the LIC located in the center, while the wireless power-charge receiving (WPRX) coil and the SFAT are placed at the top and bottom, respectively. The completed system (Fig.2b) is 18 x 18 x 38 mm³ in volume and weighs 12.56 grams (which can be adjusted by filling the inside air volume with liquid or weight, if desired), resulting in a mass density of 1.020 g/cm³.

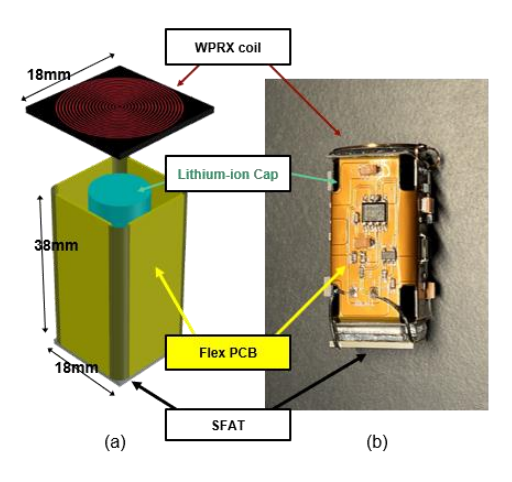


Figure 2: (a) Conceptual 3D schematic of the acoustic propeller and (b) photo of the completed acoustic propeller. Lithium-ion capacitor (LIC) cannot be seen in the photo as it is wrapped by the flexible printed circuit board (PCB).

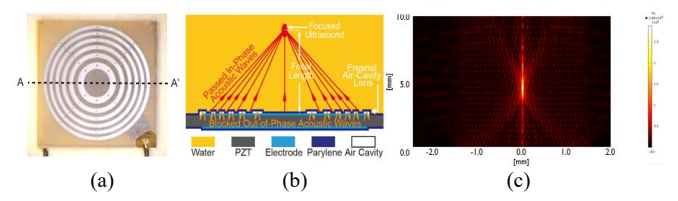


Figure 3: (a) Top-view photo of SFAT showing six air-cavity Fresnel rings on a 1-mm-thick PZT substrate, (b) schematic view of the cross-section across the dashed line (A-A') in (a), showing the focusing principle of SFAT, and (c) a finite element method (FEM) simulation, showing 5.0, 0.1 and 1.0 mm of focal length, diameter and depth, respectively.

Propeller Design and Fabrication

Self-focusing Acoustic Transducer (SFAT) is fabricated on 1-mm-thick lead zirconate titanate (PZT) substrate sandwiched by top and bottom nickel electrode layers. The nickel layers are patterned as circles, which are aligned concentrically, with the top circle having a larger diameter to compensate the top and bottom alignment error. The transducer focuses ultrasound through the aircavity Fresnel half-wavelength band (FHWB) lens over the top electrode (Fig. 3), and the radii of the air-cavity rings are designed according to

$$R_n = \sqrt{n\lambda \left(F + \frac{n\lambda}{4}\right)} \tag{1}$$

where λ and F are ultrasound wavelength in liquid and focal length (5 mm in this case), respectively [3]. Equation 1 ensures that the path length from each ring boundary to the focal point is longer than the focal length (F) by integer multiple (n) of half wavelength (i.e., $n\lambda/2$). The air cavity annular rings on the top electrode block the acoustic waves due to the acoustic impedance mismatch between air (0.4kRayl) and liquid (over 1MRayl), while the non-air-cavity rings allow the waves to pass through, so that the waves constructively interfere at the focal point, producing magnified intensity [4]. Finite element method (FEM) simulation (Fig. 3c) shows 5.0, 0.1, and 1.0 mm of focal length, focal diameter, and focal depth, respectively.

The air-cavity Fresnel lens is made of Parylene-D with AZ5214 photoresist acting as a sacrificial layer in the brief fabrication steps for SFAT shown in Fig. 4. The sacrificial layer defines the Fresnel lens and is removed with acetone to form the

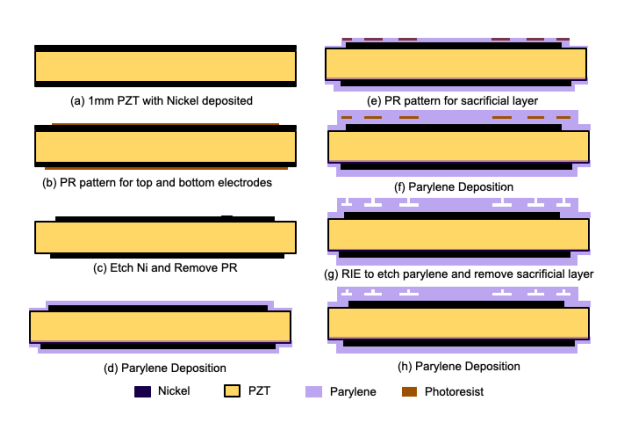


Figure 4: Brief fabrication steps of the SFAT used for the acoustic propeller.

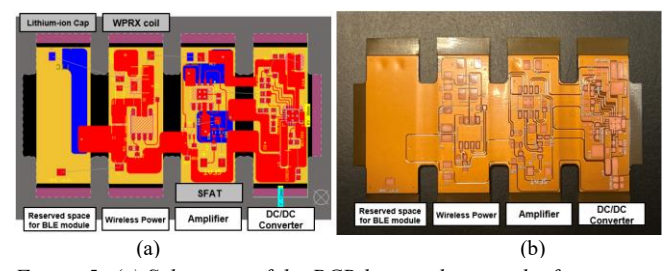


Figure 5: (a) Schematic of the PCB layout showing the four main circuits sections and the places where SFAT and LIC will be connected and (b) photo of the fabricated flexible PCB before being folded into a 3D shape shown in Fig. 2b.

air-cavity rings through release holes made on Parylene-D with O₂ Reactive Ion Etching (RIE). The release holes are sealed with another Parylene layer deposition. On a fabricated SFAT, a laser-machined acrylic sheet (2 mm thick) is glued to the opposite side of the Fresnel lens in order to form the air-cavity reflector shown in Fig. 1, so that the propulsion may be only from one side.

When a sinusoidal voltage signal with its frequency matching the PZT's thickness-mode resonance (2.32MHz for 1-mm-thick PZT) is applied between the top and bottom electrodes, the PZT effectively generates acoustic waves, which are focused through the air-cavity FHWB rings. The waves from the side of the PZT where there is no lens are blocked by the air reflector made of the acrylic sheet to prevent any propulsion from that side which would have reduced the propulsion.

Electronic Circuit Design

The drive electronics made on a flexible PCB (Fig. 5) is composed of a DC/DC converter (Texas Instruments' TPS65131), an oscillator (Analog Devices' LTC1799) for generating a square wave (1kHz - 33MHz) and a power amplifier (Texas Instruments' THS3095), as illustrated in Fig. 6. The drive electronics delivers $30V_{pp}$ 2.32MHz sinusoidal signal to the propeller when powered by a 100F lithium-ion capacitor (Xeno Energy's XLC-1030). The output of a fully charged LIC is 3.8 V_{DC} and a DC/DC converter converts the input into +/-15 V_{DC} dual outputs. The gain of the power amplifier is adjusted so that the output signal of a power amplifier may be $30V_{pp}$ 2.32MHz sinusoidal signal with sufficiently large power for the SFAT.

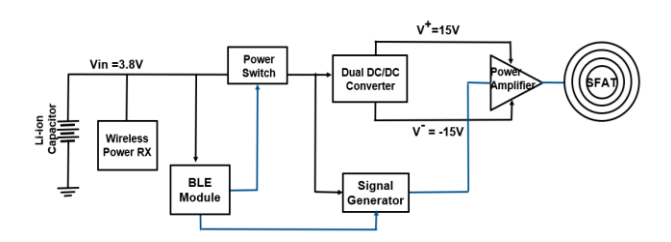


Figure 6: Functional block diagram of the circuit showing the power rails (black lines) and the signal rails (blue lines). Bluetooth low energy (BLE) module is to control the frequency and timing, and will be added in future.



Figure 7: Photos showing (a) wireless charging of LIC, while the SFAT in the propeller is immersed in water to prevent thermal damage of the SFAT during the charging and (b) air gap between transmission (TX) and receiving (RX) coils maintained by a pair of rigid wires and a clamp holding TX and RX coils, respectively, with alignment between TX and RX coils achieved by a 3-axis micromanipulation stage.

Since the SFAT requires high instantaneous power to generate the acoustic propulsion, a power source with high output power density is required. Moreover, a power source with high energy density is needed to be able to operate the acoustic propeller for sufficient time. A lithium-ion battery (LIB), which is commonly used in a portable electronic device, has high energy density but low power density. On the other hand, a super capacitor, another power source, offers a relatively high instantaneous power density but low energy density. Furthermore, a super capacitor suffers from self-discharging, which gets worse at a higher temperature. Lithium-ion capacitor (LIC) is chosen over LIB and super capacitor due to its high energy and power densities. Moreover, LIC has an extremely low self-discharging characteristic even at a high temperature. Table 1 compares LIC with super capacitor and LIB.

Table1. Comparison of lithium-ion capacitor with super capacitor and lithium-ion battery

	Super Capacitor	Lithium-ion Capacitor	Lithium-ion Battery
Energy Density	Low (< 10Wh/kg)	Medium (~10Wh/kg)	High(10 -100Wh/kg)
Power Density	Medium(1kW/kg)	High(1k -10kW/kg)	Low(~0.1kW/kg)
Operating Voltage Range	0 - 3.0V	2.2 - 3.8 V	2.5 - 4.3V
Charge/Discharge Cycle	100k	100k	500 -1000
Self Discharge	Susceptible	Very low	Very low





Figure 8: Photos of the acoustic propeller (a) floating close to the floor without acoustic propulsion and (b) soaring up to the surface of sodium polytungstate (SPT) solution (1.15g/cm³) when the SFAT generates the acoustic propulsion.

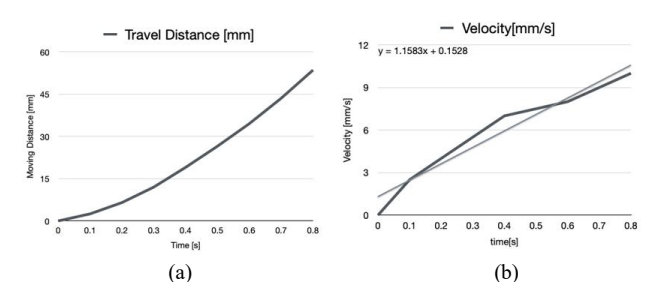


Figure 9: (a) Measured traveling distance (in mm) and (b) velocity (in mm/s) of the acoustic propeller from the vertical propulsion shown in Fig. 8. The traveling distance is measured in every 100ms and the averaged acceleration is calculated to be 1.16 mm/s²

The chosen 100F LIC is capable of delivering enough power and energy to the acoustic propeller to generate the acoustic propulsion in the water to make the propeller propagate stably for several minutes. The LIC is fully discharged before assembling the components for the propeller, in order to prevent potential damage to the SFAT (in air) due to the power from the LIC. After assembling all the components, 20µm thick Parylene is conformally deposited over all the surface of the assembled acoustic propeller to make the unit immersible in liquid. The LIC is wirelessly charged (with Taida Century Technology's T3168) through a wireless charging receiver (WPRX) coil (3- layers, $26\mu H$, 1.1A, $520m\Omega$ max) on the top of the assembled propeller unit, as shown in Fig. 7. The current flowing through the wireless charging coils is limited to 700mA to avoid potential damage to the Parylene layer due to excessive heat when the air-gap between the transmitting and receiving coils is less than 1mm.

EXPERIMENT RESULTS

Vertical Propulsion

For testing and quantifying the acoustic propulsion, the mass density of liquid solution is adjusted to be 1.15g/cm^3 by adding sodium polytungstate (SPT) powder into deionized water (DI water) at a weight ratio of 1:4.89 (SPT:water) such that the acoustic propeller sinks down close to the floor without generating any propulsion but still floats above the floor (Fig. 8a). The acoustic propeller floating in the liquid experiences the gravitational force downward as well as the upward buoyancy F_B

$$F_B = \rho g V \tag{2}$$

where ρ , g and V are the mass density of liquid, gravitational constant, and object volume, respectively. As buoyancy is a function of the density of liquid, the position of the acoustic

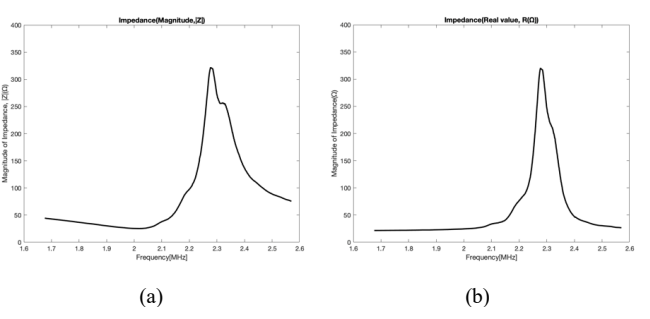


Figure 10: Measured (a) impedance magnitude and (b) resistance portion of the impedance of the SFAT immersed in SPT solution, as a function of frequency.



Figure 11: Photo of the acoustic propeller floating horizontally on sodium polytungstate (SPT) solution (1.20g/cm³).

propeller can be adjusted by changing the mass density of SPT solution.

When the SFAT generates acoustic propulsion upward, the propeller soars up to the surface of the liquid (Fig. 8b). With a continuous sinusoidal signal driving the propeller, the signal amplitude decreases gradually after being at 30 V_{pp} for 1.5 minutes, due to the LIC running out of energy, and when the amplitude becomes lower than 18 V_{pp}, the acoustic propulsion stops, after which the propeller still moves due to inertia for a while.

The acceleration of the vertical propulsion is obtained through measuring the traveling distance as a function of time (Fig. 9). From the acceleration, the acoustic propulsion force is calculated to be 18.68µN, when the LIC is fully charged, ignoring the friction and drag forces that resist the motion of the acoustic propeller.

The electrical power P_E consumed by the SFAT can be calculated with

$$P_E = \left(\frac{V_{rms}^2}{|z|^2}\right) \times R \tag{3}$$

 $P_E = \left(\frac{V_{rms}^2}{|Z|^2}\right) \times R \tag{3}$ where V_{rms}, \underline{Z} , and R are the root-mean-square (rms) voltage, SFAT's impedance, and the real part of the impedance, respectively. To measure the SFAT's impedance, we measure SFAT's one-port reflection coefficient S₁₁ with a network analyzer (Hewlett-Packard's 8753D) while SFAT is immersed in the same SPT solution, and calculate the impedance, Z (=R+jX), using

$$Z = 50 \Omega \times \frac{1 + S_{11}}{1 - S_{11}} \tag{4}$$

The impedance magnitude |Z| and resistance R of the SFAT at its resonant frequency, which is measured as 2.27MHz, are 321.61 and 319.89 Ω , respectively (Fig. 10). However, at the 2.32MHz which the electronic circuit generates and delivers to the SFAT, |Z| and R are measured as 256.09 and 209.10 Ω , respectively. Thus, the electrical power is to be 358.70mW, and the propulsion force per electrical power consumption by the SFAT is 52.07 µN/W.

Horizontal Propulsion

To move the acoustic propeller horizontally, SPT powder is added to DI water at a weight ratio of 1:3.54, resulting in the SPT solution's mass density being 1.20g/cm³ which leads to the acoustic propeller floating on the top surface of the solution while the SFAT part is still immersed in the solution as shown in Fig. 11. Since some portion of the acoustic propeller is exposed to the air, it experiences more drag force than the vertical movement. Also, as it is tilted with an angle of 27° on the surface, only 89% (cos27°) of acoustic propulsion contributes to the lateral motion.

Another way of estimating the acoustic propulsion is using a drag force. An object moving at a velocity, v, in a fluidic media experiences a drag force F_d

$$F_d = \frac{1}{2}\rho v^2 A C_d \tag{5}$$

 $F_d=\frac{1}{2}\rho v^2AC_d \eqno(5)$ where ρ,A and C_d are the liquid density, cross-sectional area, and drag constant, respectively. When the acoustic propeller travels with the constant velocity, the acoustic propulsion force is equal to the drag force so that there is zero net force, leading to no

acceleration. With the measured steady-state velocity of the acoustic propeller moving horizontally at 6 mm/s, the drag force F_d is calculated to be 11.51 µN. The calculated acoustic propulsion in the horizontal motion using the steady-state drag is smaller than that of the vertical propulsion because the propeller receives lower voltage and power from the LIC by the time when the acoustic propeller reaches the steady-state velocity.

SUMMARY

This paper presents a wireless acoustic propeller based on a self-focusing acoustic transducer (SFAT) powered by lithium-ion capacitor (LIC), particularly on the design and implementation of the propeller and its drive electronics along with the integrated system which includes the LIC power source. Also, experimental results in both vertical and horizontal propulsions have been demonstrated and characterized in sodium polytungstate solution with mass density of 1.15 - 1.20 g/cm³. The wireless acoustic propeller (18 x 18 x 38 mm³ in volume and 12.56 grams in weight) integrates all the SFAT-based propeller, dive electronics and power source. And a 2.32 MHz sinusoidal signal is obtained from the integrated signal generator, and amplified to 30 V_{pp} through the power amplifier powered by ±15 V_{DC} which is produced through the DC/DC converter from 3.8 V_{DC} of the LIC integrated in the acoustic propeller and wirelessly charged while the SFAT is immersed in liquid. When the 30 V_{pp} is applied to the propeller, it generates the maximum acoustic propulsion of 18.68µN, while the SFAT is measured to consume 358.70mW.

ACKNOWLEDGEMENTS

This paper is based on the work supported by National Science Foundation under grant ECCS2017926.

REFERENCES

- [1] R. Du, Z. Li, K. Youcef-Toumi, and P. Valdivia y Alvarado, eds. "Robot fish: Bio-inspired fishlike underwater robots," Springer, 2015.
- [2] L. Zhao and E.S. Kim, "Subminiature Underwater Propeller with Electrical Controllability of Steering," 2021 IEEE International Ultrasonics Symposium, 2021 pp. 1-4, doi: 10.1109/IUS52206.2021.9593504.
- [3] K. Yamada, H. Shimizu, "Planar-Structure Focusing Lens for Acoustic Microscope", Journal of the Acoustical Society of Japan (E), vol.12, no.3, pp.123-129, 1991
- [4] J. Lee and E.S. Kim, "Phase Array Ultrasonic Transducer Based on a Flip Chip Bonding with Indium Solder Bump," IEEE International Ultrasonics Symposium, Symposium, September 11 - 16, 2021

CONTACT

*J. Lee, tel: +1-206-902-8988; lee172@usc.edu